

Dynamic process of anti-Stokes photoluminescence at a long-range-ordered $\text{Ga}_{0.5}\text{In}_{0.5}\text{P}/\text{GaAs}$ heterointerface

Takashi Kita and Taneo Nishino

Department of Electrical and Electronics Engineering, Faculty of Engineering, Kobe University, 1-1 Rokkodai, Nada, Kobe 657, Japan

C. Geng, F. Scholz, and H. Schweizer

4. Physikalisches Institut, Universität Stuttgart, D-70550 Stuttgart, Germany

(Received 1 October 1998; revised manuscript received 28 December 1998)

Efficient anti-Stokes photoluminescence (PL) has been observed in $\text{Ga}_{0.5}\text{In}_{0.5}\text{P}$ and GaAs single heterostructure. PL of $\text{Ga}_{0.5}\text{In}_{0.5}\text{P}$ was observed when photoexciting the $\text{Ga}_{0.5}\text{In}_{0.5}\text{P}/\text{GaAs}$ interface. The anti-Stokes PL intensity from the $\text{Ga}_{0.5}\text{In}_{0.5}\text{P}$ layer is about 1% of the GaAs PL. The observed anti-Stokes PL exhibits a characteristic intensity dependence in the double-logarithmic plot, which reveals two straight lines having slopes of about 2 and 4. Time-resolved measurements show that the anti-Stokes PL is described by two components: the rapid decay caused by the two-step two-photon absorption of the excitation laser light and the slower decay by energy transfer of electron-hole recombination energy in the GaAs. We found that many-particle effects in the GaAs under high excitations cause the characteristic intensity dependence of the anti-Stokes PL. [S0163-1829(99)05323-0]

I. INTRODUCTION

Anti-Stokes photoluminescence (PL) or energy up-conversion in solids has gathered much attention in fields of optoelectronic devices. Generally, an existence of a hot reservoir in solids thermally populates carriers for momentum conserving bulk Auger process¹⁻⁴ or phonons for anti-Stokes shifts of Raman lines.^{5,6} In the bulk Auger process, energy released by electron-hole recombination is transferred to second electron or hole. The excited carriers are redistributed within their band or into another band and dissipate the energy by emission of phonons. During the energy relaxation, radiative recombination of these carriers with thermalized ones in the opposite band is possible. This gives rise to anti-Stokes PL above the band-gap energy. On the other hand, nonlinear optics in crystals up convert an incident photon energy, which are well known such as second-harmonic generation, optical parametric oscillation, and two-photon absorption via real or virtual states.⁷⁻⁹

There are some reports about anti-Stokes PL in bulk and heterostructures of semiconductors.¹⁰⁻¹³ Especially, relatively high-efficiency anti-Stokes PL have been found in semiconductor heterostructures such as InP/AlInAs,¹⁴ CdTe/ $\text{Cd}_{0.6}\text{Mg}_{0.4}\text{Te}$,¹⁵ and long-range-ordered (LRO) $(\text{Al}_x\text{Ga}_{1-x})_{0.5}\text{In}_{0.5}\text{P}/\text{GaAs}$ (Refs. 16-20) heterostructures. In these cases, the heterostructures consist of stacked narrow and wide gap semiconductors. When photoexciting the narrow gap material, excited carriers are redistributed into the wide gap material and recombination in the wide gap material generates anti-Stokes PL. Its efficiency depends on (1) excitation and carrier transfer processes from the narrow gap material into the wide gap material and (2) properties of their final states. A high efficiency of the anti-Stokes PL at the type-II InP/AlInAs heterojunction¹⁴ was verified by the cold Auger effect described by Zegrya and Kharchenko.²¹ The presence of a heteroboundary lifts the \mathbf{k} -conservation re-

quirement in the direction perpendicular to the interface and allows Auger recombination without a thermal threshold. On the other hand, low-temperature anti-Stokes PL from CdTe/ $\text{Cd}_{0.6}\text{Mg}_{0.4}\text{Te}$ quantum wells were explained by a two-step two-photon absorption (TS-TPA) mechanism via localized exciton states or via excitons bound to impurities.¹⁵ In the TS-TPA, the first photon generates carriers and the second photon pumps the generated carriers into the wide gap material. For LRO- $\text{Ga}_{0.5}\text{In}_{0.5}\text{P}/\text{GaAs}$ structures, on the other hand, cold Auger^{16,18} and TS-TPA mechanisms^{19,20} were proposed. These different mechanisms seem to explain the observed anti-Stokes PL at the LRO- $\text{Ga}_{0.5}\text{In}_{0.5}\text{P}/\text{GaAs}$ heterointerface. However, there is no unified understanding of the detailed mechanism occurred at the interface.

In this paper, we focus our attention on dynamic process of anti-Stokes PL at a LRO- $\text{Ga}_{0.5}\text{In}_{0.5}\text{P}/\text{GaAs}$ heterointerface. Time-resolved measurements revealed that the anti-Stokes PL is described by two components: the rapid decay and the slower decay limited by GaAs PL. The first step in the anti-Stokes process is excitation of the GaAs. In the second excitation step, the TS-TPA process by the excitation laser causes the rapid decay component and the energy transfer of the excess energy released by the electron-hole recombination in the GaAs causes the slower decay component. We discuss a role of many-particle effects of the GaAs in the anti-Stokes PL.

II. EXPERIMENTS

The sample used in this study is a $[\bar{1}11]$ -ordered $\text{Ga}_{0.5}\text{In}_{0.5}\text{P}$ alloy grown by low-pressure metal-organic vapor-phase epitaxy.²² The sample was grown on a (001) GaAs substrate misoriented 6° off towards $[111]_B$ at 720°C . The growth rate was $2.0 \mu\text{m/h}$ at an input gas-flow ratio of $f(\text{V})/f(\text{III})$ of 240. The layer thickness is $2 \mu\text{m}$. The order parameter can be estimated by the valence-band splitting en-

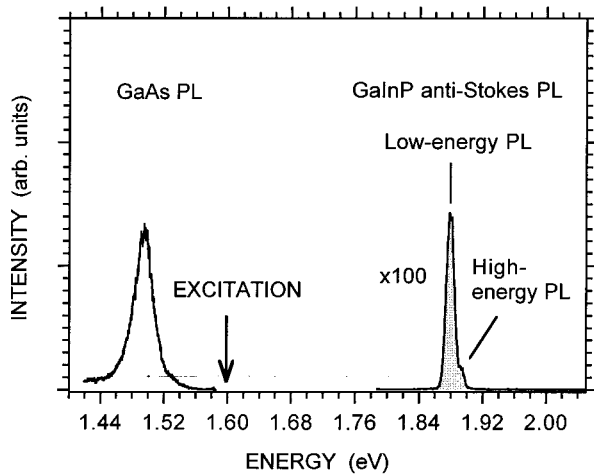


FIG. 1. PL spectrum of LRO- $\text{Ga}_{0.5}\text{In}_{0.5}\text{P}/\text{GaAs}$ excited at 1.6 eV. The intensity of the anti-Stokes PL is about 1% of the intensity of GaAs PL.

ergy, because the spin-orbit splitting and the crystal-field splitting are functions of order parameter.²³ Conventional PL-excitation (PLE) spectra were measured by a lock-in detection system under excitation by a monochromatic light of a Xe lamp. PLE spectrum shows two excitonic absorption maxima corresponding to the valence-band splitting. The measured valence-band splitting is 22 meV, which yields order parameter η of 0.44 for this sample. Ultrafast laser spectroscopy was performed using 100-fs pulses from a mode-locked Ti:sapphire laser with a repetition rate of 80 MHz. The laser wavelength is 775 nm. The incident direction of the laser light was normal to the (001) surface, and the emitted luminescence was detected at the same direction. The PL is dispersed in a 0.25-m spectromator and detected with a spatial and temporal resolution of 0.15 nm and about 5 ps due to dispersion in the collection optics, respectively, by a streak camera with two-dimensional readout. The sample was mounted in a He-gas-flow cryostat. The sample temperature was 2.7 K.

III. EXPERIMENTAL RESULTS

A. Anti-Stokes PL at LRO- $\text{Ga}_{0.5}\text{In}_{0.5}\text{P}/\text{GaAs}$ heterointerface

Figure 1 shows a time-integrated anti-Stokes PL spectrum of the LRO- $\text{Ga}_{0.5}\text{In}_{0.5}\text{P}/\text{GaAs}$. The arrow indicates the excitation-photon energy. The anti-Stokes PL intensity is about 1% of the GaAs PL. The spectrum of the anti-Stokes PL shows two peaks that will be referred to as the “high-energy” and “low-energy” PL lines. The high-energy PL is weak in the time-integrated spectrum, because of a rapid decay of its intensity. This point will be discussed in the next subsection. The excitation intensity dependence of the anti-Stokes PL is shown in Fig. 2. To make clear a behavior of the high-energy PL, we plot the spectra integrated in a time range of 0-200 ps. The spectra were normalized by the intensity of the low-energy PL. The high-energy PL line does not show an excitation intensity dependence except for its intensity. Whereas the high-energy PL line exhibits all features typical for band-to-band recombination, the low-energy PL line shifts to higher emission energies with increasing

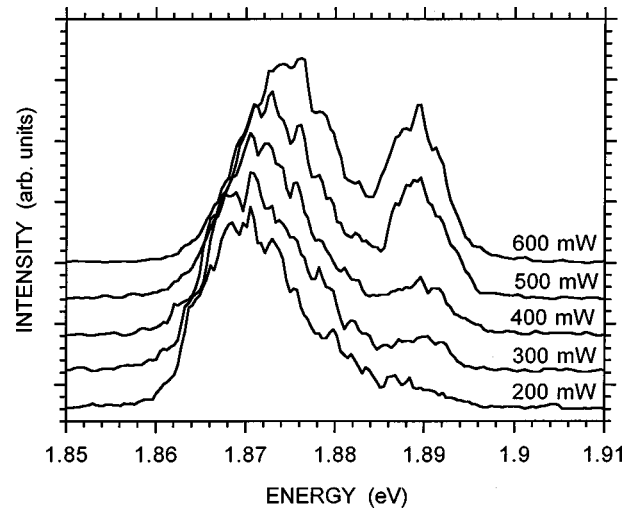


FIG. 2. Anti-Stokes PL spectra measured at various excitation intensity. These spectra are integrated in a time range of 0-200 ps. The spectra were normalized by the intensity of the low-energy PL.

excitation intensity. In addition, the temporal decay dynamics of the low-energy PL is nonexponential, which is consistent with the results of PL excited by an above-gap light.²² All these properties of the low-energy PL line can be consistently explained by assuming spatially indirect recombination. The enhancement of the high-energy PL intensity by increasing excitation intensity is stronger than that of the low-energy PL. In this paper we focus our attention on the high-energy PL corresponding to the band-to-band transition.

GaAs PL measured at various excitation intensities are shown in Fig. 3. The inset in Fig. 3 compares spectra obtained from $\text{Ga}_{0.5}\text{In}_{0.5}\text{P}$ with different order parameters. The samples with $\eta=0.0$ and 0.30 were grown at 810 and 660°C, respectively. These spectra were measured at 600 mW. The spectrum from the $\text{Ga}_{0.5}\text{In}_{0.5}\text{P}$ ($\eta=0.0$) on the GaAs shows two peaks. The peaks at 1.518 eV and 1.496 eV of the $\text{Ga}_{0.5}\text{In}_{0.5}\text{P}$ ($\eta=0.0$) sample are due to the band-to-band transition and transitions related to deeply localized states. The 1.496 eV peak becomes dominant in the samples with large-order parameter, as shown in the inset of Fig. 3.

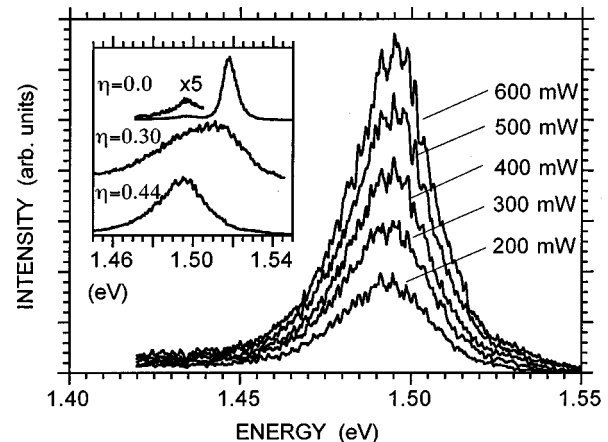


FIG. 3. GaAs PL spectra measured at various excitation intensities. The inset compares spectra obtained from $\text{Ga}_{0.5}\text{In}_{0.5}\text{P}$ with different order parameters. The excitation intensity for the inset was 600 mW.

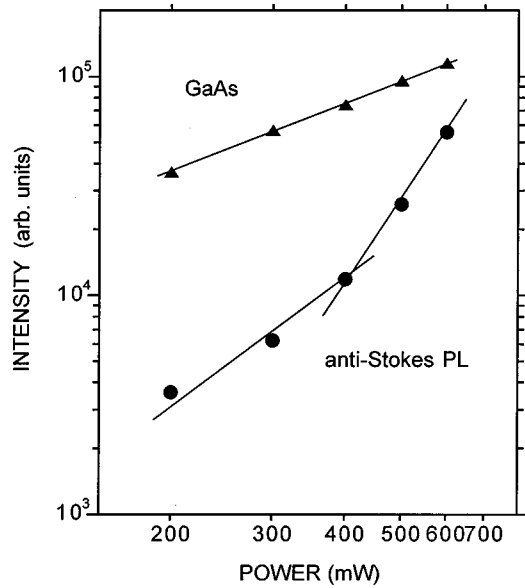


FIG. 4. Excitation intensity dependence of spectrally integrated intensities of the anti-Stokes PL and the GaAs-PL.

This indicates that the initial stages of atomic ordering strongly affect the confined electronic states at the interface. The full width at the half-maximum of the GaAs PL obtained from the sample ($\eta=0.44$) is 30 meV in the 100 mW excitation.

Figure 4 shows the spectrally integrated intensities of the anti-Stokes PL and the GaAs PL versus excitation intensity. The double-logarithmic plot for the anti-Stokes PL indicates two linear regressions. The slopes are nearly 2 and 4 for intensities below and above 400 mW, respectively. In this intensity region the GaAs PL exhibits a linear dependence on the excitation intensity. Hence, the data in Fig. 4 displays the intrinsic intensity dependence of the anti-Stokes PL. When we excite the sample by an above-gap light (2.54 eV), both PL from the $\text{Ga}_{0.5}\text{In}_{0.5}\text{P}$ and the GaAs indicate linear relationships for excitation intensity.

B. Time-resolved spectroscopy of anti-Stokes PL and GaAs PL

Decay profiles of the high-energy line of the anti-Stokes PL are shown in Fig. 5 as a function of excitation intensity. The decay profiles are described by two components: the rapid decay and the slower decay. With increased excitation intensity, the rapid decay component becomes dominant. This result indicates that the enhanced increase of the anti-Stokes PL above 400 mW excitation is caused by the increase of this rapid decay component. The time constant of this rapid component τ_r is about 100 ps. This value agrees well with the previous result of an initial decay time attributed to a rapid capture of excitons into some nonradiative deep centers in $\text{LRO-Ga}_{0.5}\text{In}_{0.5}\text{P}$.²⁴ The slower component τ_s yields a time constant of about 450 ps. To compare the decay profile time-resolved PL of the GaAs were measured. Figure 6 plots the results of the GaAs PL decays measured at 200, 300, 400, 500, and 600 mW. The decay profile is affected by excitation intensity. Above 400 mW the time constant is about 700 ps. On the other hand, below 400 mW the time

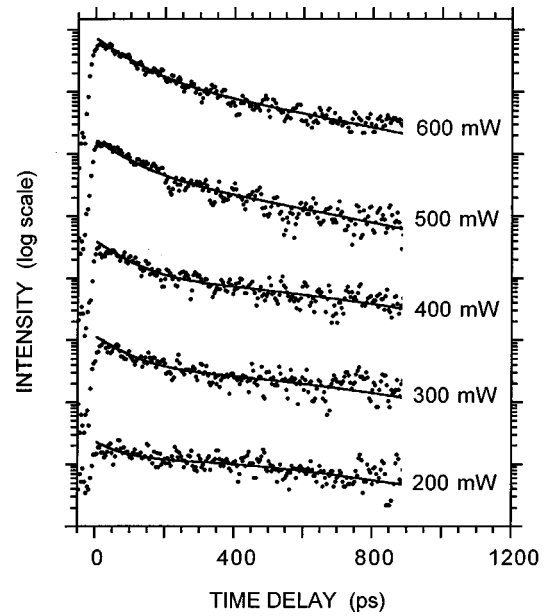


FIG. 5. Decay profiles of the anti-Stokes PL measured at various excitation intensities.

constant is about 1240 ps. The solid lines plot a simple exponential decay of 1240 ps. Since the excited carrier density at 100 mW is 10^{16} cm^{-3} , many-particle effects should be considered. If we highly excite the sample, excitons lose their identity as individual quasiparticles and a new collective phase is formed which is known as the electron-hole plasma (EHP). The critical density (Motto density) at which the EHP starts to exist is about $4 \times 10^{16} \text{ cm}^{-3}$ for GaAs at carrier temperature of 70 K.²⁵ This critical density is close to the excitation densities in our measurements. The decrease of the time constant observed in the over 400 mW excitation

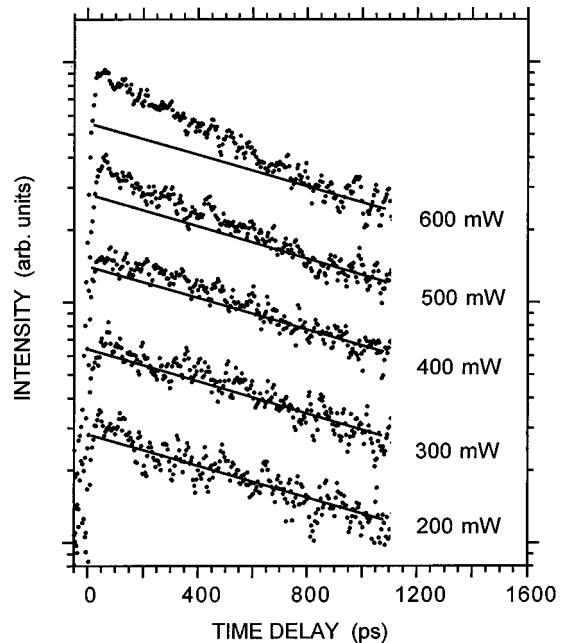


FIG. 6. Decay profiles of the GaAs PL measured at various excitation intensities. The solid lines indicate a simple exponential decay of 1240 ps.

corresponds to loss of excitonic properties. This critical intensity (400 mW) coincides with the excitation intensity showing the change in the characteristic intensity dependence in Fig. 4.

IV. DISCUSSIONS

A. The rapid decay component

The first step of the anti-Stokes process is photogeneration of electron and hole pairs in the GaAs layer. The excited carriers can be excited once again by other photons. In the second excitation step, the photons can be provided by the excitation laser or by the GaAs PL. The time constant of the GaAs PL is more than 700 ps. This is too long to compare with the rapid component, $\tau \cong 100$ ps, of the anti-Stokes PL. Thus, the laser pulse excites carriers in the second excitation step. This is a TS-TPA process by the excitation laser. In the following we show that the TS-TPA process via localized states is a possible explanation consistent with the rapid decay. In the first step, the excitation laser generates electron-hole pairs in the GaAs. After the initial excitation step electrons and holes relax down to localized states near the interface and establish a quasiequilibrium distribution. This causes the broad band PL in Fig. 3. Since the localized states have a very limited spatial extension, the electron and hole wave functions have contributions from all \mathbf{k} states in the Brillouin zone. Therefore, these long-lived electrons and holes localized near the interface can be excited to the high-energy states by the second photon absorption without phonon assistance. This scenario indicates that only limited and well-defined portion of the carriers near the interface can contribute to the second absorption process. These excited carriers into the $\text{Ga}_{0.5}\text{In}_{0.5}\text{P}$ recombine radiatively giving rise to the observed anti-Stokes PL. For high excitation, the excitonic properties of the deep localized bound states are lost and the system must be considered in terms of separate electrons and holes. However, for low excitation the system is excitonic and direct photon absorption from deep, localized bound exciton states to higher energy exciton states, having a well-defined wave vector, is possible. This excitonic process was observed in $\text{CdTe}/\text{Cd}_{0.6}\text{Mg}_{0.4}\text{Te}$ quantum wells.¹⁵

The TS-TPA model by the excitation laser consistently explains the character of the rapid decay component. Within this TA-TPA model, the electron density N_r^e fed into the $\text{Ga}_{0.5}\text{In}_{0.5}\text{P}$ is proportional to the population N_{int} of the intermediate states and to the number of photons responsible for the second absorption step. Since N_{int} of the band-to-trap process is supposed to be proportional to the excitation laser intensity,³ N_r^e is proportional to I^2 , where I is excitation laser intensity. Similarly, for the holes N_r^h is proportional to I^2 . Thus, the anti-Stokes PL intensity obeys $N_r^e N_r^h$ and hence, I^4 . On the other hand, in the excitonic model under a relatively weak excitation the anti-Stokes PL intensity obeys I^2 .¹⁵ It is considered that the critical excitation intensity between the I^4 and I^2 dependencies is 400 mW.

B. The slower decay component

The decay time of about 450 ps for the slower decay component is longer than a time constant (about 310 ps) of radiative recombination of excitons in the $\text{Ga}_{0.5}\text{In}_{0.5}\text{P}$. Hence,

a much slower second process limits the slower decay. A TS-TPA and an Auger process caused by the GaAs PL are probable processes for the slower decay component of the anti-Stokes PL. A time evolution of the anti-Stokes PL caused by the GaAs PL is given by

$$\int_0^t f(k)^l e^{-(t-k)/\tau} dk, \quad (4.1)$$

where $f(k)$ is a function of the GaAs decay profile, and τ is the radiative recombination lifetime in the $\text{Ga}_{0.5}\text{In}_{0.5}\text{P}$. l is an exponent depending on the excitation process from the GaAs into the $\text{Ga}_{0.5}\text{In}_{0.5}\text{P}$.

First we consider the Auger process. Generally in bulk materials, a hole-hole-electron (hhe) Auger process and an electron-electron-hole (eeh) process are possible. The hhe-Auger process generates holes in another band such as the split-off valence band. In contrast to this, the eeh-Auger process lifts electrons within the conduction band. This leads to a weak luminescence continuum at the higher energy side of the edge luminescence. For heterostructures of semiconductors, the presence of a heteroboundary lifts the \mathbf{k} -conservation requirement in the direction perpendicular to the interface and allows Auger recombination without a thermal threshold.²¹ In this case, contributions of the eeh- and hhe-Auger processes should be considered. If one of these processes causes the anti-Stokes PL, its excitation intensity dependence is similar to that of bulk materials.³ This will be realized at the type-II interface. Seidel *et al.*¹⁴ have found high-efficiency anti-Stokes PL at an InP/AlInAs type-II interface. Auger-excited holes recombine with thermalized conduction-band electrons in the InP . The intensity of the anti-Stokes PL has shown a dependence on I^2 . In the case of $\text{LRO-Ga}_{0.5}\text{In}_{0.5}\text{P}/\text{GaAs}$ heterostructures, degree of ordering changes the type of the $\text{Ga}_{0.5}\text{In}_{0.5}\text{P}/\text{GaAs}$ interface. With increased order parameter, the interface changes from the type I to the type II. According to a calculation,²⁶ the interface of our sample ($\eta=0.44$) is the type I. The calculated conduction- and valence-band discontinuities of the $\text{LRO-Ga}_{0.5}\text{In}_{0.5}\text{P}(\eta=0.44)/\text{GaAs}$ interface are 72 and 351 meV, respectively. Then, for the anti-Stokes PL both electron and hole should be excited into the $\text{Ga}_{0.5}\text{In}_{0.5}\text{P}$ layer at this heterointerface.

The electron N_r^e and hole N_r^h densities excited by the Auger process are given by $n^2 p$ and $p^2 n$, respectively, when we consider band-to-band process. Here, n and p are electron and hole densities excited in the GaAs, respectively. Since the anti-Stokes PL intensity is proportional to $N_r^e N_r^h$, its intensity depends on $n^3 p^3$, and hence, on I^3 . However, no clear evidence of this excitation intensity dependence was observed in Fig. 4. On the other hand, if the excitonic recombination process is dominant in the GaAs, anti-Stokes PL by the excitonic Auger process shows a dependence on I^2 .

The TS-TPA by the GaAs PL can be considered in the similar model discussed in the above subsection. The photons provided by the GaAs PL can excite carriers especially localized near the interface, because of their large range of \mathbf{k} value in the Brillouin zone. In this process the excitation intensity dependence for the slower decay component is the same as the dependence of the rapid decay component.

The decay profiles of the anti-Stokes PL are analyzed taking into account a simple exponential decay for the rapid decay component and Eq. (4.1) for the slower decay component. Typical results of a least square fit of the experimental data are shown as full lines in Fig. 5. In these fittings we used $f(k)$ obtained from Fig. 6 and τ of 310 ps. When we take $l=4$ (the TS-TPA process) for the data upon 500 and 600 mW excitations and $l=2$ (the excitonic process of the TS-TPA or the Auger) for the data upon 200, 300, and 400 mW excitations, the calculations show good agreements with the experimental data. These results suggest that the two linear regressions for densities below and above 400 mW in Fig. 4 reflect many-particle effects in the GaAs.

V. CONCLUSIONS

Dynamic process of efficient anti-Stokes PL at $\text{Ga}_{0.5}\text{In}_{0.5}\text{P}$ and GaAs single heterostructure has been investigated. The anti-Stokes PL intensity from the $\text{Ga}_{0.5}\text{In}_{0.5}\text{P}$ layer is about 1% of the GaAs PL. The observed anti-Stokes PL exhibits a characteristic intensity dependence. The double-logarithmic

plot for the anti-Stokes PL indicates two linear regressions. The slopes are nearly 2 and 4 for intensities below and above 400 mW, respectively. Time-resolved measurements show that the anti-Stokes PL is described by two components: the rapid decay caused by the two-step two-photon absorption of the excitation laser light and the slower decay by energy transfer of electron-hole recombination energy in the GaAs. We found that many-particle effects in the GaAs cause the characteristic intensity dependence of the anti-Stokes PL.

ACKNOWLEDGMENTS

We would like to acknowledge fruitful discussion with M. Oestreich of Philipps-Universität Marburg, J. Weber and H.-J. Queisser of Max-Planck-Institut, and K. Yamashita of Kobe University. This work was supported by the Photonics Materials Laboratory Project of the Graduate School of Science and Technology at Kobe University, and in part by the Scientific Research Grant-in-Aid for Scientific Research Grants Nos. 09305020 and 09750018 from the Ministry of Education, Science, and Culture, Japan.

-
- ¹R. Conradt and W. Waidelich, Phys. Rev. Lett. **20**, 8 (1968).
²K. Betzler, Solid State Commun. **15**, 1837 (1974).
³G. Benz and R. Conradt, Phys. Rev. B **16**, 843 (1977), and references therein.
⁴B. Sermage, D. S. Chemla, D. Sivco, and A. Y. Chom, IEEE J. Quantum Electron. **QE-22**, 774 (1986).
⁵R. Rudon, Adv. Phys. **13**, 423 (1964).
⁶*Light Scattering in Solids I; Introductory Concept*, 2nd ed., edited by M. Cardona, Topics in Applied Physics Vol. 8 (Springer, Berlin, 1983).
⁷For example, A. Yariv and P. Yeh, *Optical Waves in Crystals* (Wiley, Toronto, 1984).
⁸For example, Y. R. Shen, *The Principle of Nonlinear Optics* (Wiley, New York, 1984).
⁹L. G. Quagliano and H. Nather, Appl. Phys. Lett. **45**, 555 (1984), and references therein.
¹⁰E. Gornik, T. Y. Chang, T. J. Bridges, V. T. Nguyen, J. D. McGee, and W. Müller, Phys. Rev. Lett. **40**, 1151 (1978).
¹¹P. Vagos, P. Boucaud, F. H. Julien, J.-M. Lourtios, and R. Paniel, Phys. Rev. Lett. **70**, 1018 (1993).
¹²E. F. Schubert and K. Plook, J. Phys. C **18**, 4549 (1985).
¹³M. Potemski, R. Stepniewski, J. C. Maan, G. Martinez, P. Wyder, and B. Etienne, Phys. Rev. Lett. **66**, 2239 (1991).
¹⁴W. Seidel, A. Titkov, J. P. André, P. Voisin, and M. Voos, Phys. Rev. Lett. **73**, 2356 (1994).
¹⁵R. Hellmann, A. Euteneuer, S. G. Hense, J. Feldmann, P. Thomas, E. O. Göbel, D. R. Yakovlev, A. Waag, and C. Landwehr, Phys. Rev. B **51**, 18 053 (1995).
¹⁶F. A. J. M. Driessen, Appl. Phys. Lett. **67**, 2813 (1995).
¹⁷K. Yamashita, T. Kita, and T. Nishino, J. Appl. Phys. **84**, 359 (1998).
¹⁸F. A. J. M. Driessen, H. M. Cheong, A. Mascarenhas, S. K. Deb, P. R. Hageman, G. J. Bauhuis, and L. J. Giling, Phys. Rev. B **54**, R5263 (1996).
¹⁹J. Zeman, G. Martinez, P. Y. Yu, and K. Uchida, Phys. Rev. B **55**, R13 428 (1997).
²⁰Y.-H. Cho, D. S. Kim, B.-D. Choe, H. Lim, J. I. Lee, and D. Kim, Phys. Rev. B **56**, R4375 (1997).
²¹G. G. Zegrya and V. A. Kharchenko, Zh. Éksp. Teor. Fiz. **101**, 327 (1992) [Sov. Phys. JETP **74**, 173 (1992)].
²²P. Ernst, C. Geng, F. Scholz, and H. Schweizer, Phys. Status Solidi B **193**, 213 (1996).
²³S.-H. Wei, D. B. Laks, and A. Zunger, Appl. Phys. Lett. **62**, 1937 (1993).
²⁴T. Kita, M. Sakurai, K. Bhattacharya, K. Yamashita, T. Nishino, C. Geng, F. Scholz, and H. Schweizer, Phys. Rev. B **57**, R15 044 (1998).
²⁵C. F. Kingshirm, *Semiconductor Optics* (Springer, Berlin, 1997).
²⁶S. Froyen, A. Zunger, and A. Mascarenhas, Appl. Phys. Lett. **68**, 2852 (1996).